Acta Crystallographica Section B
Structural Science
ISSN 0108-7681

Bis(hfac)-copper(II) complexes bridged by pyrimidines showing magnetic interactions

Masanori Yasui, Yoshimitsu Ishikawa, Takayuki Ishida, Takashi Nogami and Fujiko Iwasaki*

Department of Applied Physics and Chemistry, The University of Electro-Communications, Chofu, Tokyo 182-8585, Japan

Correspondence e-mail: fuji@pc.uec.ac.jp

Received 13 March 2001
Accepted 14 August 2001

Crystals of bis(1,1,1,5,5,5-hexafluoropentane-2,4-dionato)bis-pyrimidinecopper(II) (1), bis(1,1,1,5,5,5-hexafluoropentane-2,4-dionato)bis(4-methylpyrimidine)copper(II) (2), bis-(1,1,1,5,5,5-hexafluoropentane-2,4-dionato)bis(quinazoline)-copper(II) (3) showed ferromagnetic interactions at extremely low temperature. Crystal structure analyses revealed that these complexes were *catena*-bis(1,1,1,5,5,5-hexafluoropentane-2,4-dionato)[μ-pyrimidine-N^1:N^3]copper(II), $[Cu(hfac)_2(pm)_2]_n$, *catena*-bis(1,1,1,5,5,5-hexafluoropentane-2,4-dionato)-[μ-4-methylpyrimidine-N^1:N^3]copper(II), $[Cu(hfac)_2(4\text{-Me-pm})]_n$, and *catena*-bis(1,1,1,5,5,5-hexafluoropentane-2,4-dionato)[μ-pyrimidine-N^1:N^3]copper(II), $[Cu(hfac)_2(qz)]_n$, for (1), (2) and (3), respectively. In (1) and (2) the pyrimidines bridge the Cu atoms with an axial–equatorial mode to form one-dimensional spiral chains. Complex (3) also forms a one-dimensional chain structure. The coordination mode of (3) is axial–axial at room temperature, while axial–equatorial at 120 K. On the other hand, the structure of the other modification of the 4-methylpyrimidine complex (4), showing paramagnetic properties, was revealed to be a trinuclei complex bridged by two 4-methylpyrimidines, tris[bis-(1,1,1,5,5,5-hexafluoropentane-2,4-dionato)copper(II)][bis-μ-4-methyl-pyrimidine-N^1:N^3]. The chain structures with an axial–equatorial coordination mode of the bridging organic moieties should play an important role in the appearance of the ferromagnetic interactions.

1. Introduction

Many organic coordination compounds containing transition metals as spin sources have been studied to develop magnetic interactions in organic compounds. Some copper(II) transition complexes, coordinated pyrimidines or related compounds which have *meta*-coordination positions, showed magnetic interactions (Ishida *et al.*, 1995, 1996, 1997). The dipyrimidine-copper(II) dinitrate complexes $Cu^{II}(NO_3)_2(pm)_3$ and $Cu^{II}(NO_3)_2(H_2O)_2(pm)_2$ (pm = pyrimidine) showed ferromagnetic and antiferromagnetic interactions, respectively. Crystal structure analyses revealed that these complexes formed one-dimensional coordination polymers bridged by pyrimidines (Yasui, Ishikawa *et al.*, 2001). The differences between the magnetic interactions depend on the coordination types of the *meta*-N atoms of the bridging pyrimidine: the axial–equatorial coordination for $Cu^{II}(NO_3)_2(pm)_3$ shows ferromagnetic interactions and the equatorial–equatorial coordination for $Cu^{II}(NO_3)_2(H_2O)_2(pm)_2$ shows antiferromagnetic interactions. Complexes of $Cu^{II}(hfac)_2$ (hfac = 1,1,1,5,5,5-hexafluoropentane-2,4-dionate) coordinated by pyrimidine (1), 4-methylpyrimidine (2) and quinazoline (3)

showed ferromagnetic interactions at extremely low temperature. In this paper structure analyses were performed on these complexes in order to elucidate the relationships between crystal structures and magnetic characters. Structural studies at low temperatures (100/120 K) were also carried out owing to the large thermal displacements of trifluoromethyl groups at room temperature. X-ray analysis revealed that the complex with 4-methylpyrimidine crystallized into two modifications, (2) and (4); the magnetic properties measured on these crystals separately showed paramagnetic properties for (4), in contrast to ferromagnetic for (2).

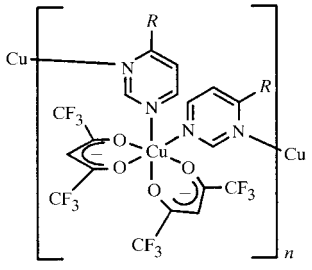

(1) R = H
(2) R = CH_3

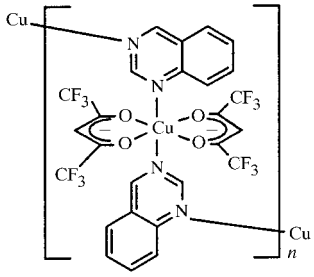

(3)

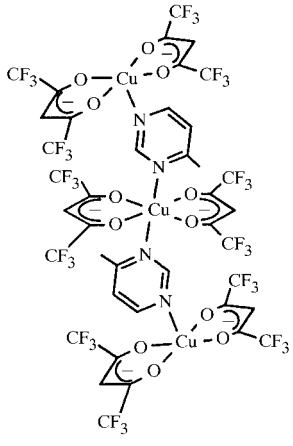

(4)

2. Experimental

Complexes (1), (2) and (3) were prepared by refluxing a dichloromethane solution of $Cu(hfac)_2$ and the bridging ligands in a stoichiometric ratio (Ishida *et al.*, 1995, 1996). The polycrystalline samples were recrystallized from dichloromethane–hexane solutions. Crystals of (2) and (4) were obtained in the same crystallization batch with different habits. These crystals were separated under the microscope and were subjected to the X-ray diffraction and magnetic studies separately. Intensity data were measured using a Rigaku AFC-7*R* diffractometer with a graphite monochromator. Intensity measurements at 120 or 100 K were carried out with an N_2 extraction gas-flow device using different crystals. The structures were solved by direct methods using the programs listed in Table 1. The H atoms at low temperatures were obtained from difference-Fourier maps. The structures were refined by full-matrix least-squares with anisotropic temperature factors for non-H atoms and isotropic ones for H atoms. For the refinements using intensity data at room temperatures, most H atoms were treated as riding models. No refinements of the disordered structures were performed, although thermal displacements of the F atoms at room temperature were very large. In the case of (1*a*) and (1*b*) refinements with the space group $I4_1/acd$, which is the higher space group of $I4_1cd$, failed. The space group $I4_1/acd$ shows a systematic abscence in the $hk0$ zone as h or $k = 2n + 1$. These reflections were rather weak, but significantly observed

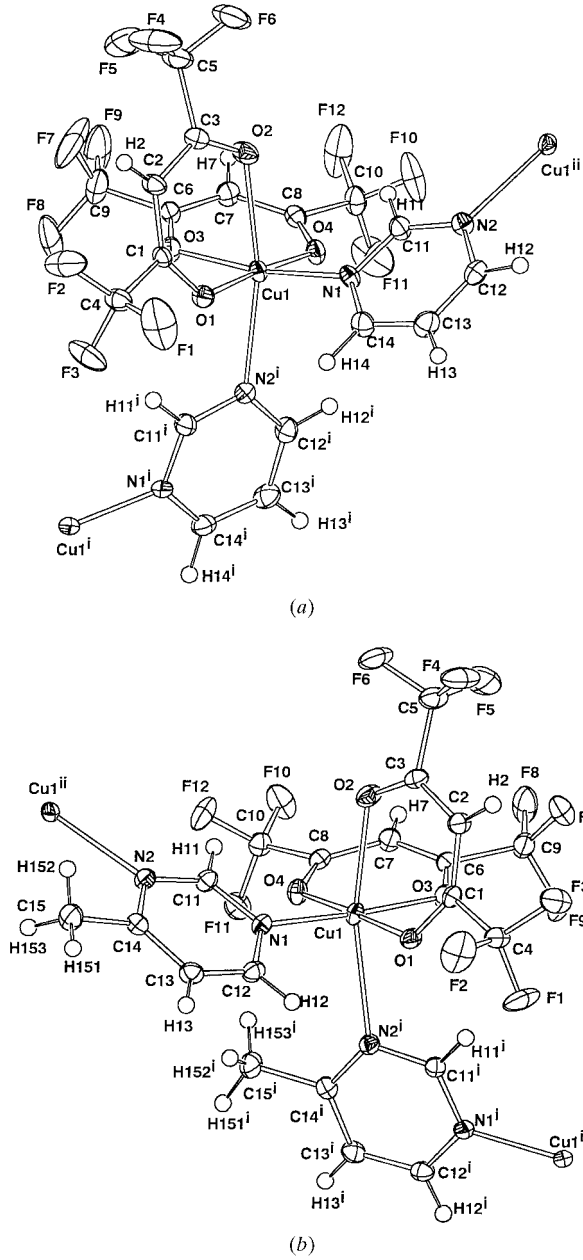

(*a*)

(*b*)

Figure 1
*ORTEP*II (Johnson, 1976) drawings of the complexes (1*b*) and (2*b*) with atom numbering. The displacement ellipsoids for the non-H atoms are drawn at 50% probability and the H atoms are drawn as spheres with a radius of 0.1 Å. (*a*) (1*b*), symmetry codes: (i) $y, \frac{1}{2}-x, \frac{1}{4}+z$; (ii) $\frac{1}{2}-y, x, z-\frac{1}{4}$. (*b*) (2*b*), symmetry codes: (i) $\frac{3}{4}-y, \frac{1}{4}+x, \frac{1}{4}+z$; (ii) $y-\frac{1}{4}, \frac{3}{4}-x, z-\frac{1}{4}$.

Table 1
Experimental details.

	(1*a*) (296 K)	(1*b*) (120 K)	(2*a*) (294 K)	(2*b*) (100 K)	(3*a*) (296 K)
Crystal data					
Chemical formula	$Cu(C_5HF_6O_2)_2$-$(C_4H_4N_2)$	$Cu(C_5HF_6O_2)_2$-$(C_4H_4N_2)$	$Cu(C_5HF_6O_2)_2$-$(C_5H_6N_2)$	$Cu(C_5HF_6O_2)_2$-$(C_5H_6N_2)$	$Cu(C_5HF_6O_2)_2$-$(C_8H_6N_2)$
Chemical formula weight	557.75	557.75	571.78	571.78	607.8
Cell setting, space group	Tetragonal, $I4_1cd$	Tetragonal, $I4_1cd$	Tetragonal, $I4_1/a$	Tetragonal, $I4_1/a$	Monoclinic, $P2_1/n$
a, b, c (Å)	18.586 (3), 18.586, 22.345 (4)	18.3757 (17), 18.3757, 22.137 (3)	19.253 (8), 19.253, 22.380 (9)	18.808 (2), 18.80, 22.182 (4)	12.300 (2), 12.1233 (18), 15.1545 (19)
β (°)	90	90	90	90	102.464 (12)
V (Å^3)	7718.9 (19)	7474.9 (12)	8296 (5)	7846.5 (16)	2206.5 (6)
Z	16	16	16	16	4
D_x (Mg m^{-3})	1.920	1.982	1.831	1.936	1.830
Radiation type	Mo $K\alpha$	Mo $K\alpha$	Mo $K\alpha$	Mo $K\alpha$	Mo $K\alpha$
No. of reflections for cell parameters	25	25	25	24	25
θ range (°)	13.3–17.4	13.2–17.4	13.5–17.4	13.1–18.7	12.5–17.3
μ (mm^{-1})	1.271	1.312	1.185	1.253	1.120
Temperature (K)	296	120	294	100	296
Crystal form, color	Pillar, green	Pillar, green	Prism, green	Prism, green	Pillar, green
Crystal size (mm)	0.35 × 0.25 × 0.25	0.330 × 0.250 × 0.250	0.20 × 0.20 × 0.20	0.30 × 0.20 × 0.20	0.30 × 0.15 × 0.10
Data collection					
Diffractometer	Rigaku AFC-7*R*	Rigaku AFC-7*R*	Rigaku AFC-7*R*	Rigaku AFC-7*R*	Rigaku AFC-7*R*
Data collection method	ω–2θ scans	ω–2θ scans	ω–2θ scans	ω–2θ scans	ω–2θ scans
Absorption correction	Psi-scan (North *et al.*, 1968)	Numerical (Coppens *et al.*, 1965)	Psi-scan	Numerical	Psi-scan
T_{min}	0.729	0.724	0.764	0.879	0.827
T_{max}	0.737	0.753	0.795	0.907	0.888
No. of measured, independent and observed parameters	2282, 2282, 1759	4317, 2210, 2008	5031, 4747, 2602	9495, 4517, 3920	5433, 5063, 2806
Criterion for observed reflections	$I > 2\sigma(I)$	$I > 2\sigma(I)$	$I > 2\sigma(I)$	$I > 2\sigma(I)$	$I > 2\sigma(I)$
R_{int}	0.0000	0.0294	0.0280	0.0253	0.0512
θ_{max} (°)	27.50	27.49	27.48	27.50	27.50
Range of h, k, l	$0 \rightarrow h \rightarrow 24$ $0 \rightarrow k \rightarrow 17$ $0 \rightarrow l \rightarrow 29$	$0 \rightarrow h \rightarrow 23$ $0 \rightarrow k \rightarrow 23$ $0 \rightarrow l \rightarrow 28$	$0 \rightarrow h \rightarrow 24$ $0 \rightarrow k \rightarrow 24$ $0 \rightarrow l \rightarrow 29$	$0 \rightarrow h \rightarrow 24$ $0 \rightarrow k \rightarrow 24$ $-28 \rightarrow l \rightarrow 28$	$-15 \rightarrow h \rightarrow 15$ $0 \rightarrow k \rightarrow 15$ $0 \rightarrow l \rightarrow 19$
No. and frequency of standard reflections	3 every 150 reflections	3 every 150 reflections	3 every 150 reflections	3 every 150 reflections	3 every 150 reflections
Intensity decay (%)	0.12	0.93	−2.41	2.06	−0.96
Refinement					
Refinement on	F^2	F^2	F^2	F^2	F^2
$R[F^2>2\sigma(F^2)]$, $wR(F^2)$, S	0.045, 0.1388, 1.071	0.0296, 0.0827, 1.055	0.0527, 0.1796, 1.028	0.0273, 0.0838, 1.082	0.0447, 0.1622, 1.023
No. of reflections and parameters used in refinement	2282, 304	2210, 322	4747, 315	4517, 339	5063, 369
H-atom treatment	Riding	Refined	Riding	Refined	Refined
Weighting scheme	$w = 1/[\sigma^2(F_o^2) + (0.0671P)^2 + 16.8141P]$, where $P = (F_o^2 + 2F_c^2)/3$	$w = 1/[\sigma^2(F_o^2) + (0.0433P)^2 + 8.5189P]$, where $P = (F_o^2 + 2F_c^2)/3$	$w = 1/[\sigma^2(F_o^2) + (0.0781P)^2 + 8.0262P]$, where $P = (F_o^2 + 2F_c^2)/3$	$w = 1/[\sigma^2(F_o^2) + (0.0456P)^2 + 3.8089P]$, where $P = (F_o^2 + 2F_c^2)/3$	$w = 1/[\sigma^2(F_o^2) + (0.0757P)^2 + 0.3712P]$ where $P = (F_o^2 + 2F_c^2)/3$
$(\Delta/\sigma)_{max}$	0.014	0.003	0.001	0.001	0.046
$\Delta\rho_{max}$, $\Delta\rho_{min}$ (e Å^{-3})	0.67, −0.378	0.595, −0.36	0.546, −0.367	0.351, −0.494	0.481, −0.414
Extinction method	None	None	None	None	Not applied

	(3*b*) (120 K)	(4*a*) (294 K)	(4*b*) (100 K)
Crystal data			
Chemical formula	$Cu(C_5HF_6O_2)_2(C_8H_6N_2)$	$Cu_3(C_5HF_6O_2)_6(C_5H_6N_2)_2$	$Cu_3(C_5H_6O_2)_6(C_5H_6N_2)_2$
Chemical formula weight	607.8	1621.2	1621.2
Cell setting, space group	Monoclinic, $P2_1/n$	Triclinic, $P\bar{1}$	Triclinic, $P\bar{1}$
a, b, c (Å)	12.023 (5), 11.920 (4), 15.065 (4)	11.728 (4), 13.621 (5), 10.919 (2)	11.552 (3), 13.397 (4), 10.505 (3)
α, β, γ (°)	90, 102.42 (2), 90	94.46 (3), 113.78 (2), 65.02 (2)	95.48 (2), 112.982 (19), 64.503 (18)

Table 1 (continued)

	(3*b*) (120 K)	(4*a*) (294 K)	(4*b*) (100 K)
V (Å^3)	2108.4 (13)	1437.8 (7)	1345.8 (6)
Z	4	1	1
D_x (Mg m^{-3})	1.915	1.872	2.000
Radiation type	Mo $K\alpha$	Mo $K\alpha$	Mo $K\alpha$
No. of reflections for cell parameters	25	24	25
θ range (°)	12.9–15.9	10.1–13.8	12.7–16.3
μ (mm^{-1})	1.172	1.275	1.362
Temperature (K)	120	294	100
Crystal form, color	Pillar, green	Pillar, green	Pillar, green
Crystal size (mm)	0.210 × 0.20 × 0.10	0.250 × 0.130 × 0.10	0.250 × 0.120 × 0.10
Data collection			
Diffractometer	Rigaku AFC-7*R*	Rigaku AFC-7*R*	Rigaku AFC-7*R*
Data collection method	ω–2θ scans	ω–2θ scans	ω–2θ scans
Absorption correction	Numerical	Psi-scan	Numerical
T_{min}	0.799	0.811	0.823
T_{max}	0.894	0.883	0.895
No. of measured, independent and observed parameters	5064, 4838, 3317	6904, 6586, 3590	6750, 6185, 5044
Criterion for observed reflections	$I > 2\sigma(I)$	$I > 2\sigma(I)$	$I > 2\sigma(I)$
R_{int}	0.0382	0.0167	0.0165
θ_{max} (°)	27.50	27.48	27.50
Range of h, k, l	$0 \rightarrow h \rightarrow 15$ $-15 \rightarrow k \rightarrow 0$ $-19 \rightarrow l \rightarrow 19$	$0 \rightarrow h \rightarrow 15$ $-16 \rightarrow k \rightarrow 17$ $-14 \rightarrow l \rightarrow 12$	$-11 \rightarrow h \rightarrow 14$ $-15 \rightarrow k \rightarrow 17$ $-13 \rightarrow l \rightarrow 12$
No. and frequency of standard reflections	3 every 150 reflections	3 every 150 reflections	3 every 150 reflections
Intensity decay (%)	2.28	8.13	2.79
Refinement			
Refinement on	F^2	F^2	F^2
$R[F^2 > 2\sigma(F^2)]$, $wR(F^2)$, S	0.0454, 0.1346, 1.023	0.0561, 0.1967, 1.028	0.0345, 0.0932, 1.026
No. of reflections and parameters used in refinement	4838, 369	6586, 430	6185, 466
H-atom treatment	Refined	Fixed	Refined
Weighting scheme	$w = 1/[\sigma^2(F_o^2) + (0.0599P)^2 + 2.1059P]$, where $P = (F_o^2 + 2F_c^2)/3$	$w = 1/[\sigma^2(F_o^2) + (0.0942P)^2 + 0.5397P]$, where $P = (F_o^2 + 2F_c^2)/3$	$w = 1/[\sigma^2(F_o^2) + (0.0418P)^2 + 1.0143P]$, where $P = (F_o^2 + 2F_c^2)/3$
$(\Delta/\sigma)_{max}$	0.000	0.007	0.008
$\Delta\rho_{max}$, $\Delta\rho_{min}$ (e Å^{-3})	1.236, −1.004	0.736, −0.426	0.62, −0.584
Extinction method	None	None	None

Computer programs used: *AFC* (Rigaku Corporation, 1994), *TEXSAN* (Molecular Structure Corporation, 1992), *SIR*92 (Altomare *et al.*, 1994), *SAPI*91 (Fan, 1991), *SHELXL*97 (Sheldrick, 1997), *ORTEP*II (Johnson, 1976).

with $I/\sigma(I) > 10$. Crystal data, details concerning data collection and structure refinements are listed in Table 1.[1]

3. Results and discussion

3.1. Structures of (1) and (2)

The molecular structures of (1*b*) at 120 K and (2*b*) at 100 K, along with the atomic numbering, are shown in Fig. 1. Selected bond distances and angles at low temperatures are listed in Table 2. For each complex, the Cu atom is coordinated by O1, O3, O4 and N1 equatorially, and N2^i [(i) $y, \frac{1}{2} - x, \frac{1}{4} + z$ for (1) and (i) $\frac{3}{4} - y, \frac{1}{4} + x, \frac{1}{4} + z$ for (2)] and O2 axially to form a six-coordinated octahedral complex. Therefore, two hfac groups coordinate the Cu atom with a *cis* configuration. The pyrimidine moiety bridges the Cu···Cu at the *meta* N atoms with equatorial and axial positions to form a one-dimensional chain. In (1*b*) the axial Cu1—O2 and Cu1—N2^i distances are 2.346 (3) and 2.387 (3) Å, respectively. The corresponding values for (2*b*) are 2.2861 (13) and 2.4957 (15) Å for Cu1—O2 and Cu1—N2^i, respectively. The longer Cu1—N^i distance of (2*b*) than (1*b*) is due to the steric effect of the methyl group. Dihedral angles related to the pyrimidine planes are also listed in Table 2. The inclination of the pyrimidine plane to the equatorial plane of (1*b*) is slightly different from that of (2*b*).

Stereoscopic views of the coordination polymer chains of (1*b*) and (2*b*) are shown in Fig. 2. In the crystals of (1) the pyrimidine groups bridge the Cu atoms to form a 4_3 spiral chain along the *c* axis. The 4_1 spiral chain is also generated from the symmetry operation of the space group. The spiral chain of (2) shown in Fig. 2 has a 4_1 symmetry. These

[1] Supplementary data for this paper are available from the IUCr electronic archives (Reference: OA0036). Services for accessing these data are described at the back of the journal.

complexes are the first bis(hfac)-Cu complexes having polymer chain structures bridged by N atoms from the result of the search of the Cambridge Structural Database (CSD; Allen & Kennard, 1993).

3.2. Structure of (3)

In the crystals of (3), two independent Cu atoms, Cu1 and Cu2, occupy the inversion centers. The structures of these complexes along with the atomic numbering are shown in Fig. 3. Selected bond distances and angles at 296 and 120 K are listed in Table 3. The coordination around the Cu atom is two *trans* hfac groups and two quinazolines. The quinazoline molecule bridges Cu1 and Cu2 at the *meta* N atoms to form a one-dimensional chain. A stereoscopic view of the coordination polymer chain of (3*b*) is shown in Fig. 4. At room temperature, the coordination lengths of Cu1—O1, Cu1—O2 and Cu1—N1 are 2.002 (2), 2.070 (3) and 2.182 (4) Å, respectively. The coordination lengths of Cu2—O3, Cu2—O4 and Cu2—N2 are 1.963 (2), 1.965 (3) and 2.464 (3) Å, respectively. For both Cu1 and Cu2 atoms, the two hfac groups coordinate equatorially and two quinazoline moieties coordinate axially. That is, the quinazoline ring bridges Cu atoms with the axial–axial coordination. The complexes showing ferromagnetic interactions with bridging *meta*-N atoms in the polymer chains, analyzed so far, have shown the axial–equatorial coordination type.

However, the coordination mode changed drastically at 120 K. The length of Cu1—N1 reduced to 2.043 (3) from 2.182 (4) Å and the length of Cu1—O2 increased to 2.189 (3) from 2.070 (3) Å. That is, the coordination of the quinazoline changes from an axial position to an equatorial one at 120 K. On the other hand, the coordination type around the Cu2

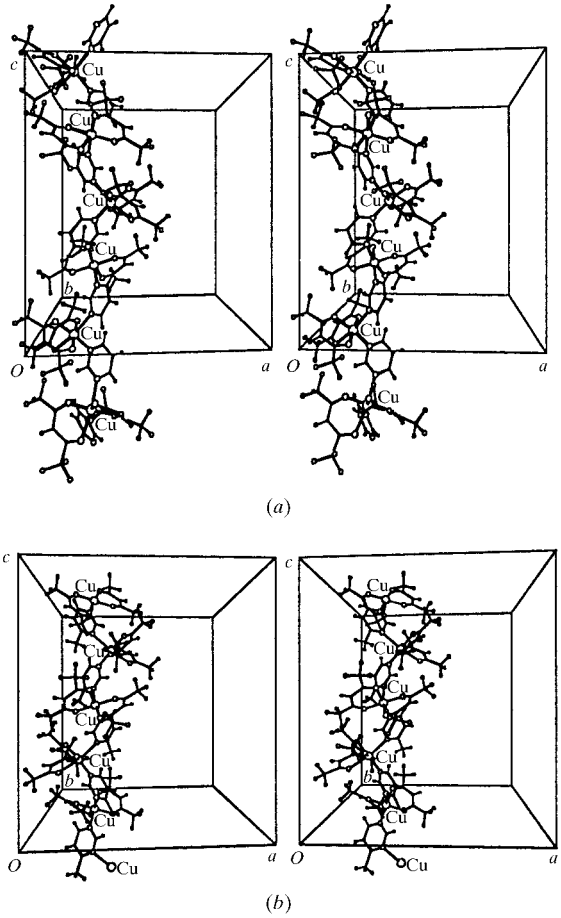

Figure 2
Stereoscopic views of the coordination polymers of (*a*) (1*b*) and (*b*) (2*b*).

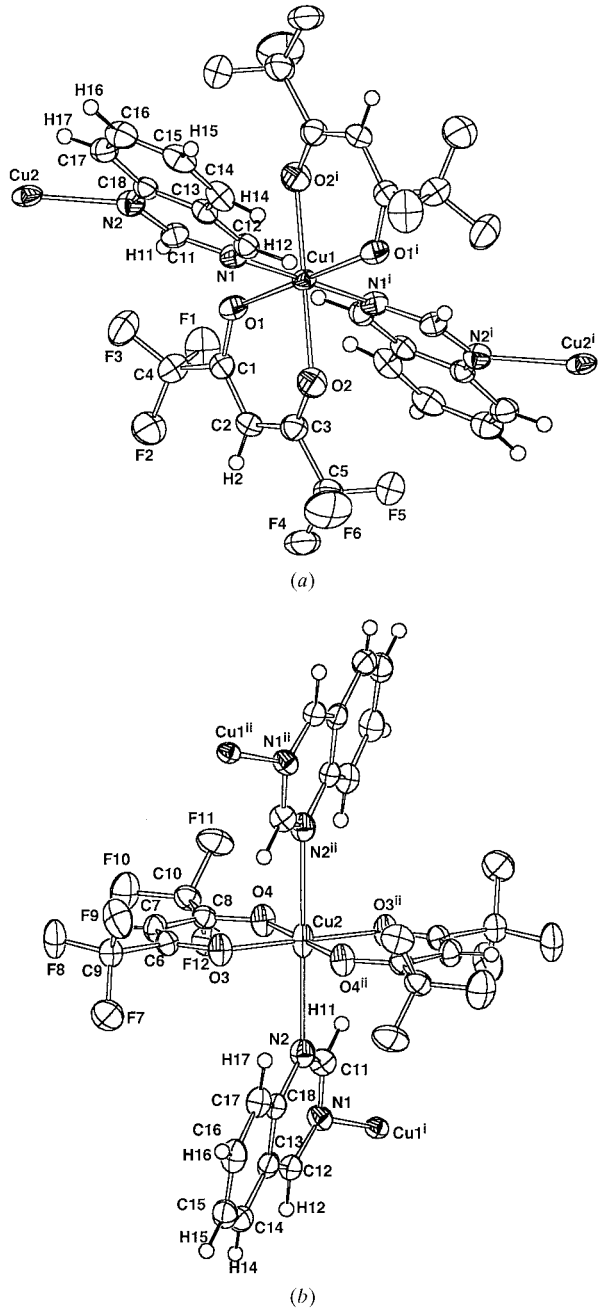

Figure 3
*ORTEP*II (Johnson, 1976) drawings of the complexes of (3*b*) with atom numbering. The displacement ellipsoids for non-H atoms are drawn at 50% probability and the H atoms are drawn as spheres with a radius of 0.1 Å. (*a*) Complex of Cu1; (*b*) complex of Cu2. Symmetry codes: (i) $-x, -y, -z$; (ii) $-x, 1-y, -z$.

Table 2
Selected bond lengths and angles (1*b*) and (2*b*) (Å, °).

	(1*b*)	(2*b*)
Cu1—O1	1.952 (3)	1.9558 (12)
Cu1—O2	2.346 (3)	2.2861 (13)
Cu1—O3	1.989 (3)	1.9970 (13)
Cu1—O4	1.949 (3)	1.9558 (12)
Cu1—N1	2.029 (4)	2.0212 (15)
Cu1—N2^{i}	2.387 (3)	2.4957 (15)
O1—Cu1—O2	86.25 (12)	87.20 (5)
O1—Cu1—O3	91.29 (12)	90.70 (5)
O1—Cu1—O4	176.22 (11)	178.24 (5)
O1—Cu1—N1	91.33 (13)	91.63 (6)
O1—Cu1—N2^{i}	84.84 (13)	82.95 (5)
O2—Cu1—O3	82.04 (11)	84.19 (5)
O2—Cu1—O4	97.24 (12)	94.49 (5)
O2—Cu1—N1	89.58 (13)	93.02 (6)
O2—Cu1—N2^{i}	167.66 (12)	166.81 (5)
O3—Cu1—O4	90.62 (13)	89.98 (5)
O3—Cu1—N1	171.04 (14)	176.28 (6)
O3—Cu1—N2^{i}	89.63 (12)	87.17 (5)
O4—Cu1—N1	87.27 (13)	87.77 (5)
O4—Cu1—N2^{i}	91.92 (13)	95.46 (5)
N1—Cu1—N2^{i}	99.14 (11)	96.00 (5)
Plane 1–pm	80.56 (11)	82.87 (4)
Plane 2–pm	37.12 (15)	31.56 (7)
Plane 3–pm	40.28 (14)	35.17 (6)
Plane 1–pm^{i}	29.44 (16)	38.29 (6)
Plane 2–pm^{i}	88.22 (10)	86.89 (12)
Plane 3–pm^{i}	78.11 (9)	76.41 (11)
pm–pm^{i}	84.82 (12)	86.52 (5)

Plane 1: Cu1—O1—C1—C2—C3—O2; plane 2: Cu1—O3—C6—C7—C8—O4; plane 3: Cu1—O1—O3—O4—N1. Symmetry codes: (i) $y, \frac{1}{2}-x, \frac{1}{4}+z$ for (1*b*); (i) $-y+\frac{3}{4}, x+\frac{1}{4}, z+\frac{1}{4}$ for (2*b*).

atom was kept during the temperature change. These facts show that the quinazoline ring bridges Cu atoms with an axial–equatorial coordination mode at 120 K and an axial–axial mode at room temperature. The axial–equatorial coordination is favored to the appearance of the ferromagnetic interaction observed at extremely low temperature.

Preliminary measurements showed gradual changes of the lattice constants from 296 to 100 K. The lattice constants, measured with some crystals which were obtained in the same crystallization batch, showed no significant change compared with the results in Table 1. Thus, all crystals in this batch are identical to each other. Detailed examinations of the structural changes and a possibility of the phase transition are in progress.

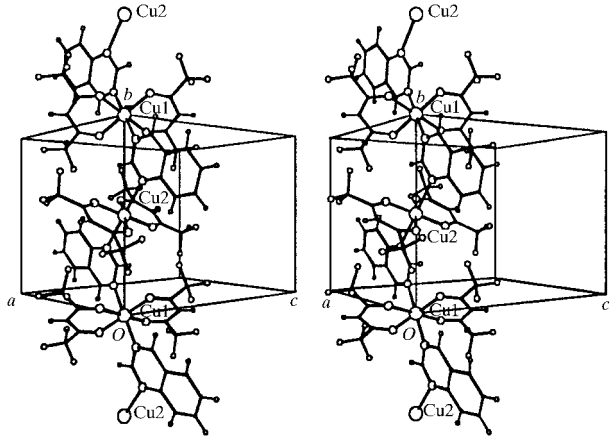

Figure 4
Stereoscopic view of the coordination polymer of (3*b*).

Table 3
Selected bond lengths and angles (3*a*) and (3*b*) (Å, °).

	(3*a*) (296 K)	(3*b*) (120 K)
Cu1—O1	2.002 (2)	2.011 (2)
Cu1—O2	2.070 (3)	2.189 (3)
Cu1—N1	2.182 (4)	2.043 (3)
Cu2—O3	1.963 (2)	1.957 (2)
Cu2—O4	1.965 (3)	1.968 (2)
Cu2—N2	2.464 (3)	2.439 (3)
O1—C1	1.247 (4)	1.272 (4)
O2—C3	1.241 (5)	1.248 (4)
O3—C6	1.245 (4)	1.260 (4)
O4—C8	1.253 (5)	1.258 (4)
N1—C11	1.363 (5)	1.364 (4)
N1—C12	1.318 (5)	1.325 (4)
N2—C11	1.295 (5)	1.308 (4)
N2—C18	1.403 (5)	1.397 (4)
O1—Cu1—O2	88.73 (11)	87.37 (9)
O1—Cu1—O2^{i}	91.27 (11)	92.64 (9)
O1—Cu1—N1	88.77 (11)	88.76 (11)
O1—Cu1—N1^{i}	91.23 (11)	91.24 (11)
O2—Cu1—N1	96.71 (13)	96.29 (11)
O2—Cu1—N1^{i}	83.29 (13)	83.71 (11)
O3—Cu2—O4	91.78 (11)	92.08 (10)
O3—Cu2—O4^{ii}	88.22 (11)	87.92 (10)
O3—Cu2—N2	91.35 (12)	91.32 (11)
O3—Cu2—N2^{ii}	88.65 (12)	88.67 (10)
O4—Cu2—N2	88.36 (11)	88.68 (10)
O4—Cu2—N2^{ii}	91.64 (11)	91.32 (10)

Symmetry codes: (i) $-x, -y, -z$; (ii) $-x, -y+1, -z$.

Table 4
Selected bond lengths and angles (4*b*) (Å, °).

Cu1—O1	1.9715 (17)	Cu2—O4	1.9393 (18)
Cu1—O2	1.9509 (17)	Cu2—O5	1.9379 (17)
Cu1—N1	2.437 (2)	Cu2—O6	1.9727 (18)
Cu2—O3	1.9578 (18)	Cu2—N2	2.225 (2)
O1—Cu1—O2	92.21 (7)	O4—Cu2—O5	169.08 (8)
O1—Cu1—O2^{i}	87.79 (7)	O5—Cu2—O6	91.82 (7)
O1—Cu1—N1	90.23 (7)	O3—Cu2—N2	100.68 (8)
O2—Cu1—N1	87.14 (7)	O4—Cu2—N2	95.99 (8)
O3—Cu2—O4	92.00 (8)	O5—Cu2—N2	94.94 (8)
O3—Cu2—O5	86.24 (7)	O6—Cu2—N2	93.66 (7)
O3—Cu2—O6	165.64 (8)		

Symmetry code: (i) $-x, -y+1, -z$.

3.3. Structure of (4)

The molecular structure of (4) along with the atomic numbering is shown in Fig. 5. Bond distances and angles are listed in Table 4. Two types of Cu atoms are located in complex (4). The Cu1 atom is located at the center of inversion of the crystals and is coordinated by two hfac groups equatorially and two bridging 4-methylpyrimidines axially, forming a six-coordinated octahedron. On the other hand, the Cu2 atom

Table 5
Summary of the structural features of Cu complexes coordinated with hfac/NO_3 and pyrimidines showing magnetic interactions.

Complexes	Structure	$(hfac)_2$ coordination	*meta*-N coordination	Magnetic interaction	Atoms in eq. plane	Bond lengths (Å)			
						eq. Cu—N	eq. Cu—O	ax. Cu—N	ax. Cu—O
(1) $(hfac)_2(pm)_2$[a]	Polymer	*Cis*	Ax.–eq.	Ferromagnetic	3O 1N	2.029	1.963	2.387	2.346
(2) $(hfac)_2$(4-Me-pm)$_2$[a]	Polymer	*Cis*	Ax.–eq.	Ferromagnetic	3O 1N	2.021	1.970	2.496	2.286
(3) $(hfac)_2(qz)_2$ [a]	Polymer	*Trans*	Ax.–eq.	Ferromagnetic	2O 2N	2.043	2.011		2.189
		Trans			4O		1.963	2.439	
(4) $(hfac)_2$(4-Me-pm)$_2$[a]	Trinuclei	*Trans*	Ax.–ax.	Paramagnetic	4O		1.961	2.437	
		Trans			4O		1.952	2.225	
$(NO_3)_2(pm)_3$[b]	Polymer		Ax.–eq.	Ferromagnetic	2O 2N	2.030	1.990	2.293	
$(NO_3)_2(pm)_2(H_2O)_2$[b]	Polymer		Eq.–eq.	Antiferromagnetic	2O 2N	2.032	2.011		2.340
$(NO_3)_2(pm)_2(H_2O)_2$[b]	Mononucleus		Unbridged	Paramagnetic	2O 2N	2.017	1.973		2.435

References: (*a*) this work; (*b*) Yasui, Ishikawa *et al.* (2001).

occupying a general position is located at the center of the base of the five-coordinated square pyramid, formed by two equatorial hfac groups and a bridging pyrimidine. The Cu2 atom deviates from the plane formed by the four O atoms of the hfac groups to the N2 atom by 0.2149 (9) Å. This deviation is also shown from the large bond angles of N2—Cu2—O. The whole structure of the complex is a trinuclei metal complex bridged by two pyrimidines. The lengths of axial Cu—N bonds are 2.437 (2) and 2.225 (2) Å for Cu1—N1 and Cu2—N2, respectively. The plane formed by Cu1 and O atoms of two hfac groups (plane 1), the plane formed by Cu2 and O atoms of two hfac groups (plane 2) and the pyrimidine plane (plane 3) are orthogonal to each other with dihedral angles of 73.10 (6), 79.27 (7) and 83.51 (7)°, for planes 1–2, 1–3 and 2–3, respectively.

The crystal structure of (4) is shown in Fig. 6. In the crystals, plane 2, the base of the square pyramid, overlaps face-to-face to that at (ii) $1-x, -y, 1-z$. The mean distance between planes is 3.725 (3) Å and the distance of Cu2···Cu2^{ii} is 4.8273 (15) Å. The corresponding values at 300 K are 3.996 (6) and 5.326 (19) Å. The appearance of the paramagnetic property of (4) can be ascribed to the segregated arrangement of trinuclei Cu complexes.

Similar trinuclei Cu complexes bridged by two 5-methylpyrimidines and two 2,3,5-trimethylpyradines were searched from the CSD. The structural feature of the 5-methylpyrimidine complex is very close to that of (4), including the packing mode (Kogane *et al.*, 1994). The length of the central Cu—N bond (2.051 Å) is shorter than that of (4) and the intermolecular Cu···Cu distance (5.885 Å) is longer than that of (4). In the case of the pyradine derivative, the coordination of the hfac groups is *cis* at both terminal sides with five-coordinated square pyramids (Kogane *et al.*, 1994). The packing mode of the crystals is quite different from that of (4).

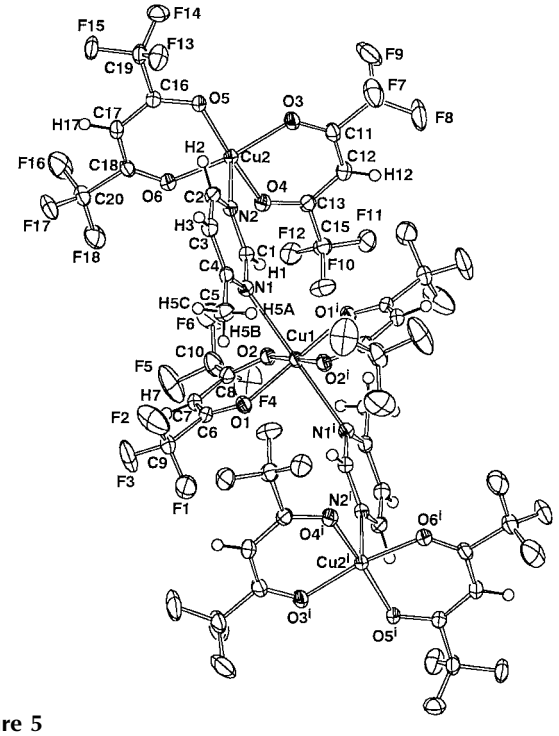

Figure 5
*ORTEP*II (Johnson, 1976) drawing of (4*b*) with atom numbering. The displacement ellipsoids for non-H atoms are drawn at 50% probability and the H atoms are drawn as spheres with a radius of 0.1 Å. Symmetry codes: (i) $-x, 1-y, -z$.

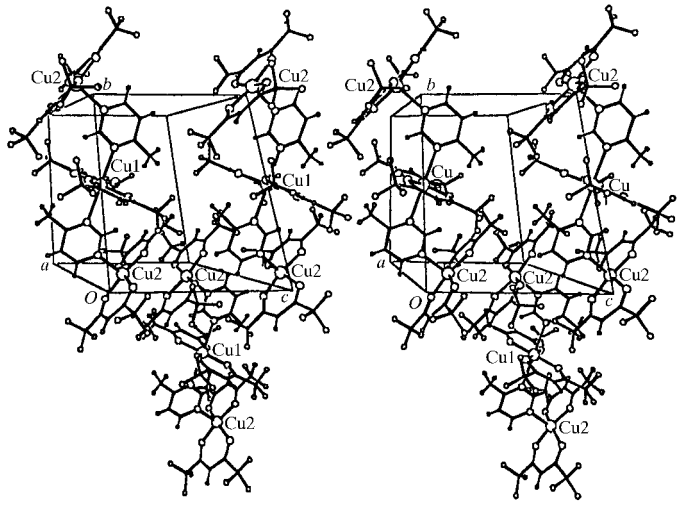

Figure 6
Stereoscopic view of the crystal structure of (4*b*).

3.4. Relations between magnetic interactions and coordination structure

The structural features of $(hfac)_2Cu^{II}$ complexes with bridging pyrimidines, as well as those of $(NO_3)_2Cu^{II}$ complexes, showing magnetic interactions are summarized in Table 5. In the crystals of the complexes showing ferromagnetic interactions (1), (2), (3) and $Cu^{II}(NO_3)_2(pm)_3$, coordination polymer chains are formed and the coordination mode of the bridging *meta* N atoms of the pyrimidine moieties is axial–equatorial. On the other hand, the coordination type of the complex, $Cu^{II}(NO_3)_2(H_2O)_2(pm)_2$, showing an antiferromagnetic interaction, is equatorial–equatorial, although the structure is a one-dimensional polymer chain. These facts indicate that the pyrimidine bridge can work as both ferromagnetic and antiferromagnetic couplers. It can be concluded that the coordination modes of the bridging *meta* N atoms play important roles to determine the differences between magnetic interactions. The electron density study on $Cu^{II}(NO_3)_2(H_2O)_2(pm)_2$ shows that an unpaired electron of the Cu^{II} ion is located in the $d_{x^2-y^2}$ orbital (Yasui, Takayama *et al.*, 2001). The magnetic coupling can be explained in terms of orbital overlaps between a molecular orbital of the pyrimidine and two Cu^{II} $d_{x^2-y^2}$ orbitals. With appreciable overlaps on both sides of the pyrimidine, the magnetic coupling is expected to be antiferromagnetic. When one N atom of pyrimidine is axially coordinated to the copper(II) ion, there is no orbital overlap between the Cu^{II} $d_{x^2-y^2}$ and N $n\sigma$ and $p\pi$ orbitals due to orthogonality (Ishida & Nogami, 1997). Thus, the axial–equatorial combination favors the ferromagnetic interaction. Therefore, it is very important that the coordination mode of (3) changes from axial–axial at room temperature to axial–equatorial at low temperature, since the magnetic interactions appear at extremely low temperature.

This work was supported in part by a Grant-in-Aid for Scientific Research (No. 08454180) and a Grant-in-Aid for Scientific Research on Priority Areas 'Molecular Conductors and Magnets' and 'Metal Assembled Complexes' (Area Nos. 730/11 224 204 and 401/11 136 212, respectively) from the Ministry of Education, Science, Sports and Culture.

References

Allen, F. H. & Kennard, O. (1993). *Chem. Des. Autom. News*, **8**, 31–37.
Altomare, A., Cascarano, M., Giacovazzo, C., Guagliardi, A., Burla, M. C., Polidori, G. & Camalli, M. (1994). *J. Appl. Cryst.* **27**, 435.
Coppens, P., Leiserowitz, L. & Rabinovich, D. (1965). *Acta Cryst.* **18**, 1035–1038.
Fan, H.-F. (1991). *SAPI*91. Rigaku Corporation,Tokyo, Japan.
Ishida, T., Mitsubori, S., Nogami, T., Ishikawa, Y., Yasui, M., Iwasaki, F., Iwamura, H., Takeda, N. & Ishikawa, M. (1995). *Synth. Met.* **71**, 1791–1792.
Ishida, T., Nakayama, K., Nakagawa, M., Sato, W., Yasui, M., Iwasaki, F. & Nogami, T. (1997). *Synth. Met.* **85**, 1655–1658.
Ishida, T. & Nogami, T. (1997). *Recent Res. Dev. Pure Appl. Chem.* **1**, 1–15.
Ishida, T., Nogami, T., Yasui, M., Iwasaki, F., Iwamura, H., Takeda, N. & Ishikawa, M. (1996). *Mol. Cryst. Liq. Cryst.* **279**, 87–96.
Johnson, C. K. (1976). *ORTEP*II. Report ORNL-5138. Oak Ridge National Laboratory, Tennessee, USA.
Kogane, T., Kobayashi, K., Ishii, M., Hirota, R. & Nakahara, M. (1994). *J. Chem. Soc. Dalton Trans.* pp. 13–18.
Molecular Structure Corporation (1992). *TEXSAN*. MSC, 3200 Research Forest Drive, The Woodlands, TX 77381, USA.
North, A. C. T., Phillips, D. C. & Mathews, F. S. (1968). *Acta Cryst.* A**24**, 351–359.
Rigaku Corporation (1994). *AFC Control Software*. Rigaku Corporation, Tokyo, Japan.
Sheldrick, G. M. (1997). *SHELXL*97. University of Göttingen, Germany.
Yasui, M., Ishikawa, Y., Akiyama, N., Ishida, T., Nogami, T. & Iwasaki, F. (2001). *Acta Cryst.* B**57**, 288–295.
Yasui, M., Takayama, R., Akiyama, N., Hashidume, D. & Iwasaki, F. (2001). *Mol. Cryst. Liq. Cryst.* In the press.